Supplemental Data

Table S1. Read number of Hippo pathway genes from RNA-sequencing of Non-IR and IR CFP+ NEPs isolated from P5 *Nestin-CFP* mice.

Gene	Non-IR NEPs	IR NEPs	Unadjusted p value
Yap	3203	3051	0.88
Taz	2129	2211	0.73
Tead1	8018	8137	0.91
Tead2	7219	7587	0.64
Tead3	648	490	0.08
Ctgf	72	86	0.50
Birc5	2687	3125	0.19
Gapdh	2081	2212	0.60

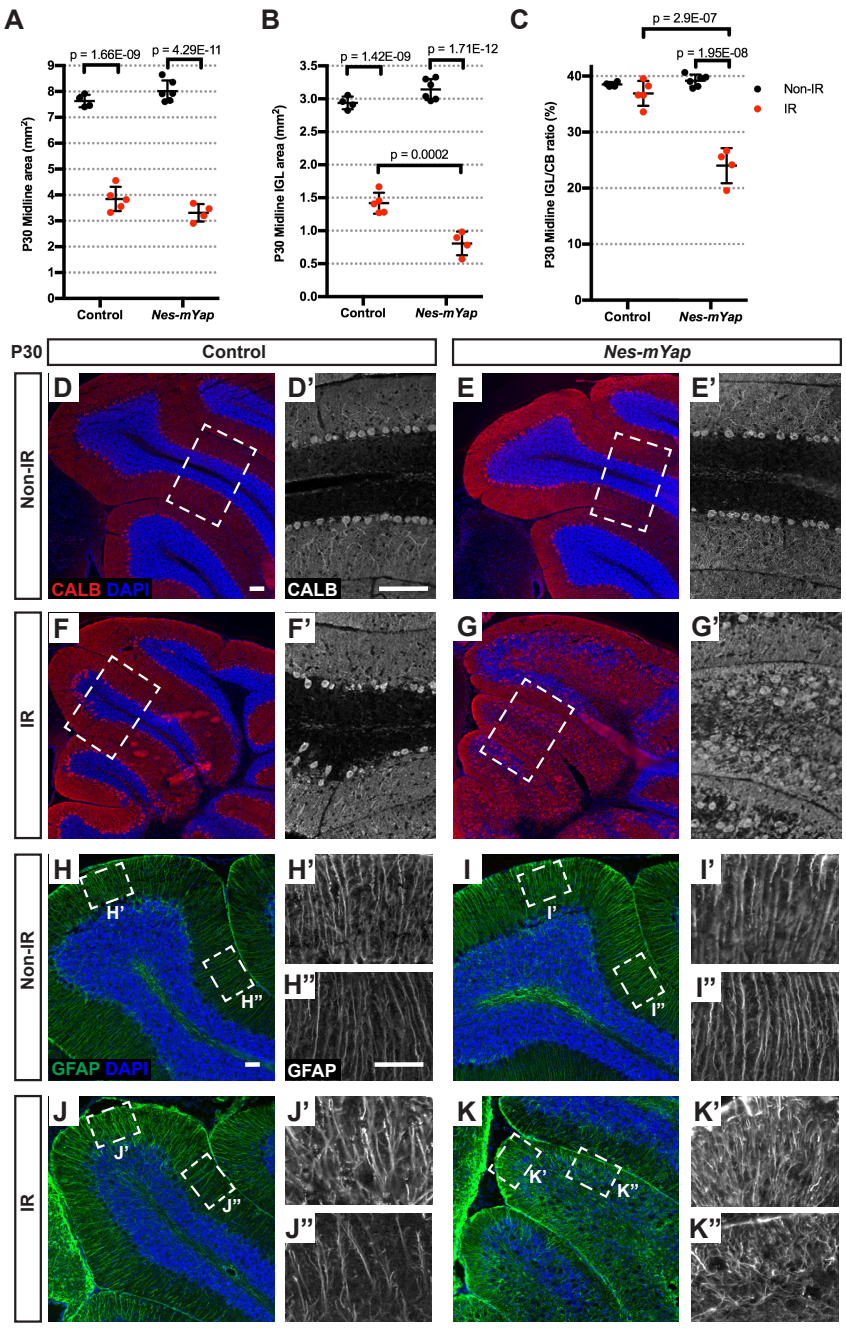

Figure 2S1. Deletion of of *Yap* in NEPs hinders injury-induced regeneration of the CB and disrupts the layered cytoarchitecture.
(A-C) Graphs of the midline cerebllar areas (A), IGL areas (B), and IGL/CB ratios (C) from *Nes-mYap* cKOs (Non-IR, n = 6; IR, n = 4) and controls (Non-IR, n = 4; IR, n = 5) at P30. Data are presented as mean ± S.D., and statistical analysis by two-way ANOVA. Each data point represents one animal. (D-K) Representative images from lobule 4/5 showing IF staining of Calbindin (CALB) (D-G) and GFAP (H-K) on midsagittal sections from *Nes-mYap* cKOs and controls at P30. (D'-G') Magnification of areas within dotted lines in D-G. (H'-K', H"-K") Magnification of areas within dotted lines in H-K. Scale bars, 50 μm.

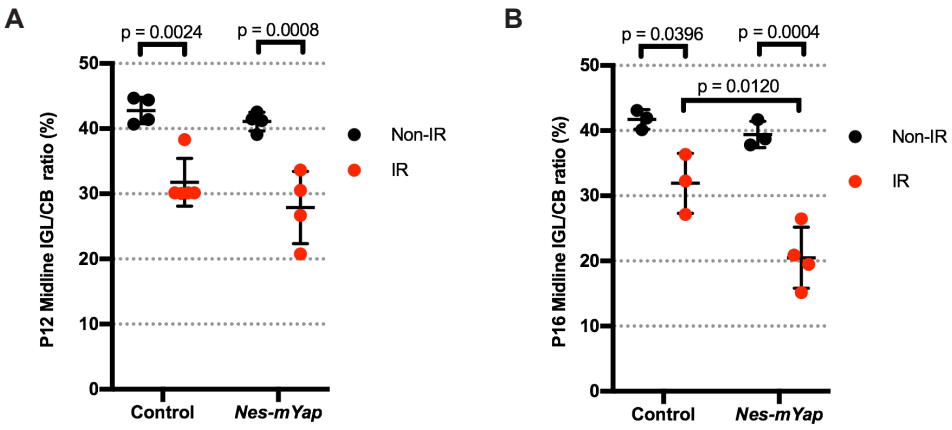

Figure 2S2. The defect in recovery of mutants lacking *Yap* in NEPs from irradiation occurs after P12.

(A-B) Graphs of the IGL/CB area ratios from *Nes-mYap* cKOs and controls at P12 (A) and P16 (B). P12 *Nes-mYap* cKO: Non-IR, n = 4; IR, n = 4; P12 control: n = 4; IR, n = 5; P16 *Nes-mYap* cKO: Non-IR, n = 3; IR, n = 3; P16 control: n = 3; IR, n = 3. Data are presented as mean ± S.D., and statistical analysis by two-way ANOVA. Each data point represents one animal.

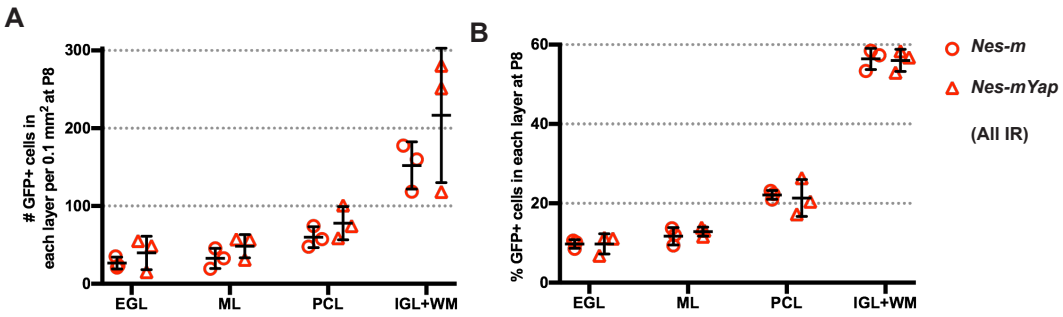

Figure 3S. Deletion of of *Yap* in NEPs does not alter the distribution of Nestin-derived cells in the different layers of the cerebellar cortex at P8 after irradiation.

Graphs of the numbers and percentages of GFP+ cells within each layer (A,B) and the total numbers of GFP+ cells (C) per 0.1 mm^2 of the total area analyzed in lobule 4/5 from midsagittal sections of IR *Nes-m* controls (n=3) and *Nes-mYap* cKOs (n = 3) at P8. Data are presented as mean ± S.D., and statistical analysis by two-way ANOVA. Each data point represents one animal.

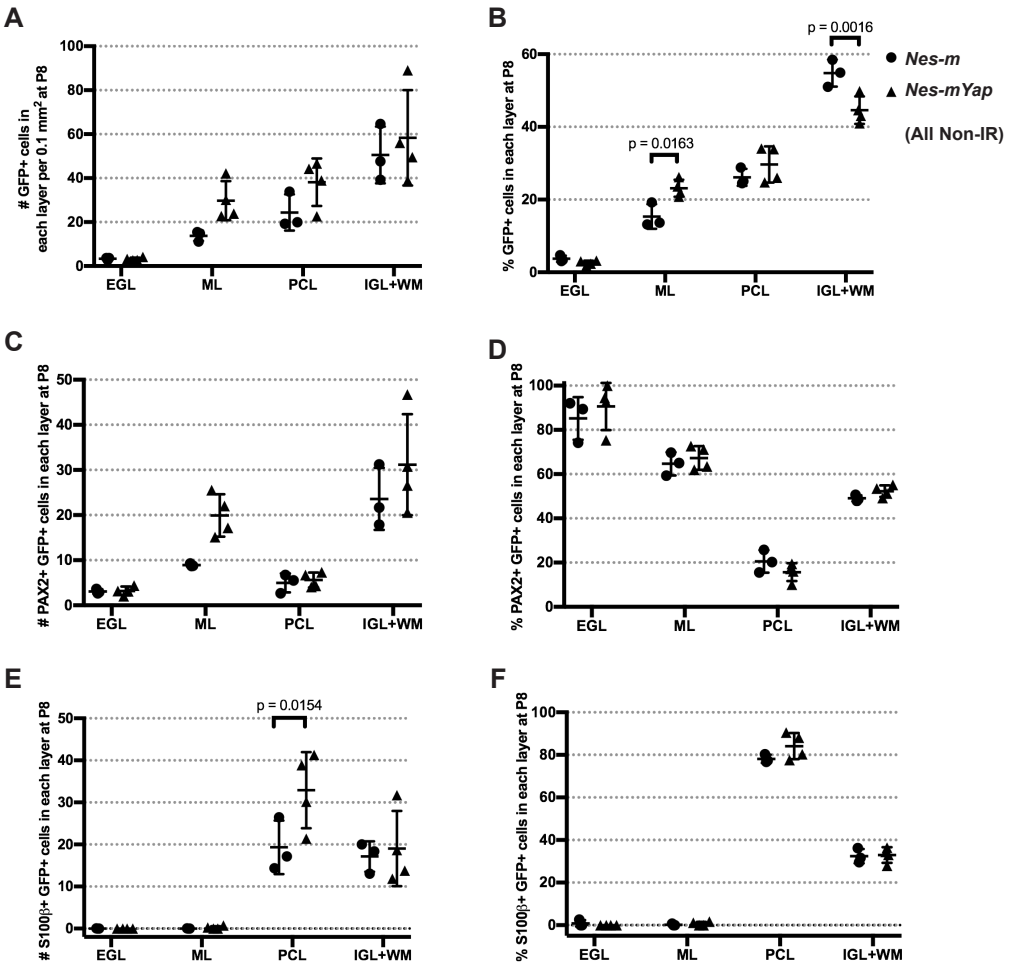

Figure 4S1. YAP promotes differentiation of NEPs during normal postnatal CB development.

Graphs of the numbers and percentages of GFP+ cells in the different layers (A,B), the numbers and percentages of PAX2+ GFP+ double cells (C,D) or S100β+ GFP+ double cells (E,F) within each layer, per 0.1 mm^2 of the total area analyzed in lobule 4/5 of midsagittal sections from *Nes-m* controls (n=3) and *Nes-mYap* cKOs (n = 4) at P8. Data are presented as mean ± S.D., and statistical analysis by two-way ANOVA. Each data point represents one animal.

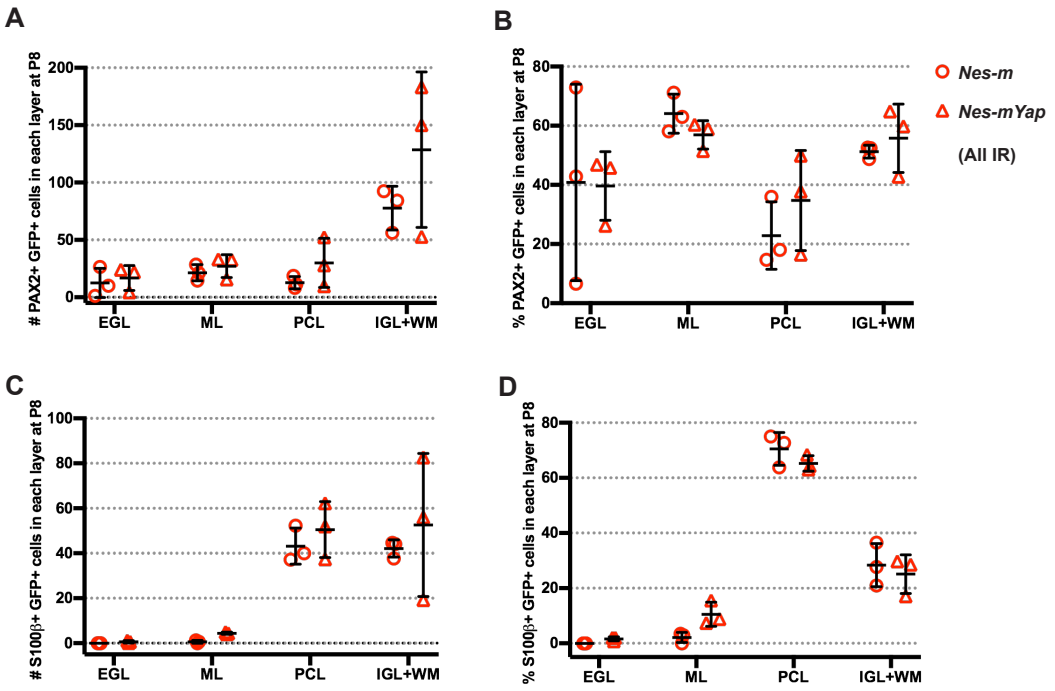

Figure 4S2. Irradiation causing depletion of the EGL overrides the requirement for YAP in differentiation of NEPs.
Graphs of the numbers and percentages of PAX2+ GFP+ double cells (A,B) or S100β+ GFP+ double cells (C,D) within each layer per 0.1 mm^2 of the total area analyzed in lobule 4/5 from midsagittal sections of IR *Nes-m* controls (n=3) and *Nes-mYap* cKOs (n = 3) at P8. Data are presented as mean ± S.D., and statistical analysis by two-way ANOVA. Each data point represents one animal.

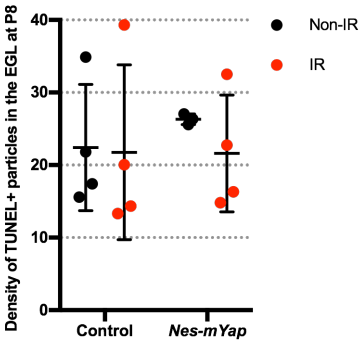

Figure 5S. Loss of YAP does not increase cell death in the EGL at P8
Graph of the densities of TUNEL+ particles in the EGL (the number of TUNEL+ particles per 0.1 mm^2 of EGL area) in midline CB sections from IR and Non-IR *Nes-mYap* cKOs and controls at P8. Controls: Non-IR, n = 4; IR, n = 4. *Nes-mYap* cKO: Non-IR, n = 3; IR, n = 4. Data are presented as mean ± S.D., and statistical analysis by two-way ANOVA. Each data point represents one animal.

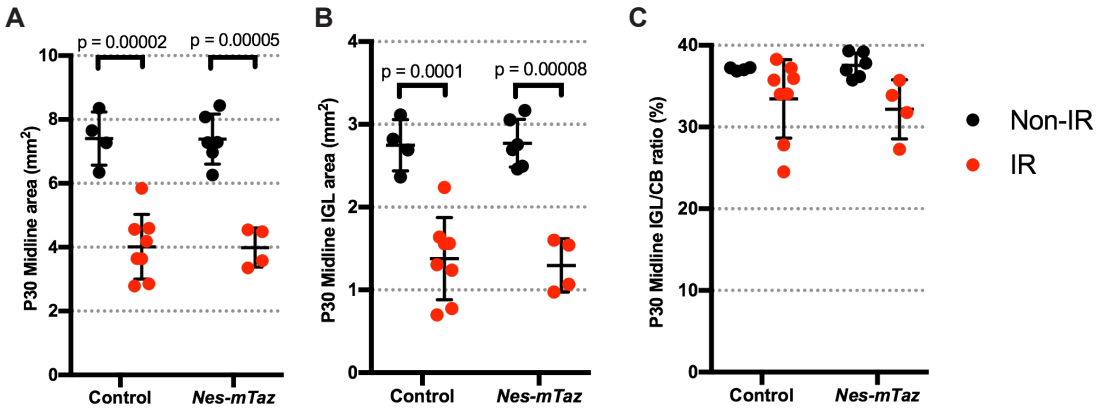

Figure 7S. Loss of *Taz* in NEPs does not affect cerebellar growth during development and regeneration.
(A-C) Graphs of the CB areas (A), the IGL areas (B), and IGL/CB area ratios (C) of midline CB sections from *Nes-mTaz* cKOs (Non-IR, n = 6; IR, n = 4) and controls (Non-IR, n = 4; IR, n = 8) at P30. Data are presented as mean ± S.D., and statistical analysis by two-way ANOVA. Each data point represents one animal.

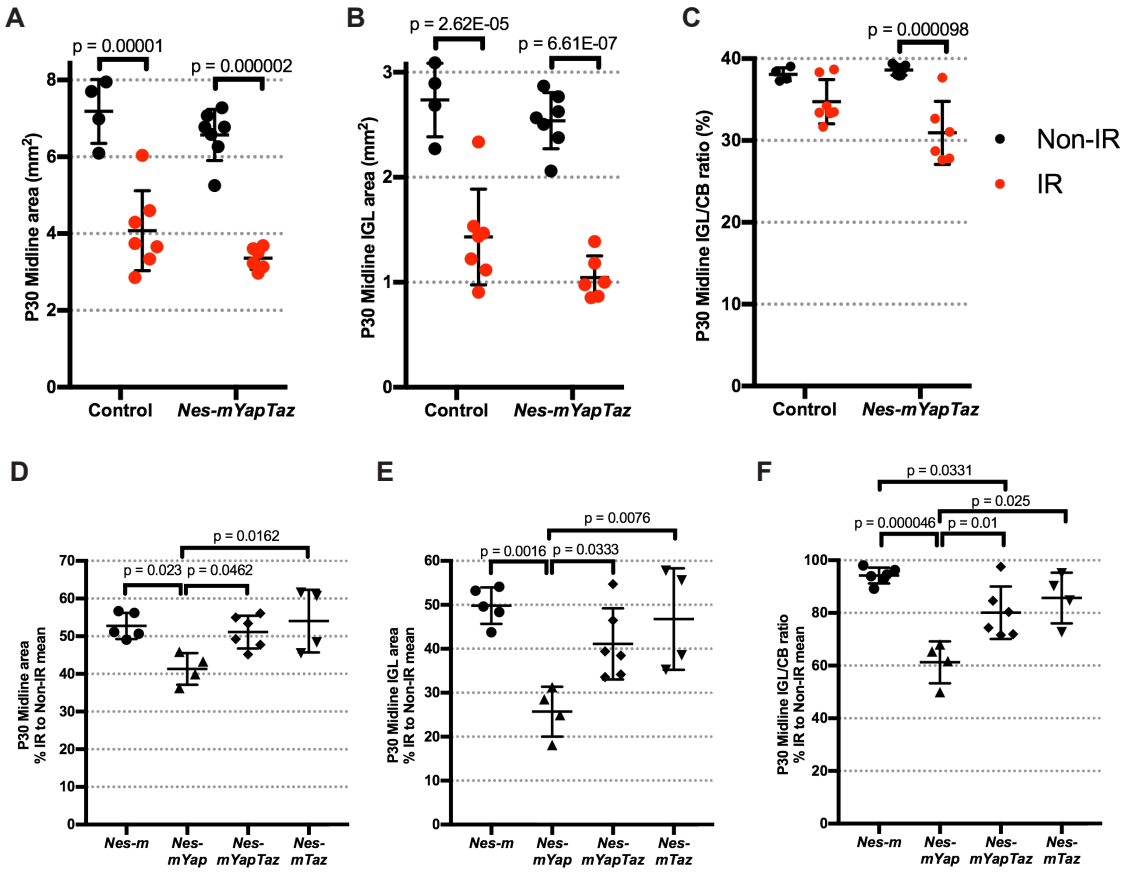

Figure 8S1. Loss of *Taz* in NEPs lacking *Yap* does not abrogate recovery of the IGL after irradiation.

(A-C) Graphs of the midline cerebellar areas (A), IGL areas (B), and IGL/CB ratios for IR and Non-IR *Nes-mYazTaz* cKOs (Non-IR, n = 7; IR, n = 6) and controls (Non-IR, n = 4; IR, n = 7) at P30. Data are presented as mean ± S.D., and statistical analysis by two-way ANOVA. Each data point represents one animal. (D-F) Graphs of the percentages of midline cerebellar areas (D), IGL areas (E), and IGL/CB ratios (F) for IR mice of the indicated genotypes as a percentage of Non-IR mice of the same genotype at P30. *Nes-m* controls (Non-IR, n = 6; IR, n = 5), *Nes-mYap* cKO (Non-IR, n = 6; IR, n = 4), *Nes-mYazTaz* cKO (Non-IR, n = 7; IR, n = 6), and *Nes-mTaz* cKO (Non-IR, n = 6; IR, n = 4). Data are presented as mean ± S.D., and statistical analysis by one-way ANOVA. Each data point represents one animal.

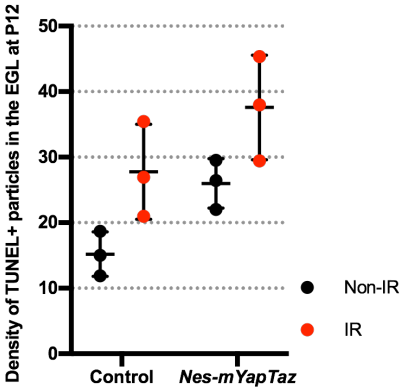

Figure 8S2. Loss of *Yap* and *Taz* in NEPs at P0 does not result in a significant increase in cell death in the EGL at P12 after irradiation-induced EGL injury at P1.

Graph of the densities of TUNEL+ particles in the EGL (the number of TUNEL+ particles per 0.1 mm^2 of EGL area) in midline cerebellar sections from IR and Non-IR *Nes-mYapTaz* cKOs and controls at P12. For all groups, n = 3. Data are presented as mean ± S.D., and statistical analysis by two-way ANOVA. Each data point represents one animal.